Journal of the Physical Society of Japan
Vol. 68, No. 9, September, 1999, pp. 2906-2909

Direct Observation of the Multiple Spin Gap Excitations in Two-Dimensional Dimer System $SrCu_2(BO_3)_2$

Hiroyuki NOJIRI, Hiroshi KAGEYAMA[1], Kenzo ONIZUKA[1], Yutaka UEDA[1] and Mitsuhiro MOTOKAWA

Institute for Materials Research, Tohoku University, Katahira 2-1-1, Sendai 980-8577
[1]*Institute for Solid State Physics, University of Tokyo, Roppongi 7-22-1, Tokyo 106-8666*

(Received June 1, 1999)

Various spin-gap excitations have been observed in the two-dimensional dimer system $SrCu_2(BO_3)_2$ by ESR. The zero-field energy gap of the lowest spin-gap excitation shows a splitting into two triplet modes and the energy splitting clearly depends on the magnetic field orientation. A zero-field splitting is also found between the $S_z = +1$ and $S_z = -1$ branches of each triplet. These behaviors are qualitatively explained by considering the anisotropic inter-dimer and intra-dimer exchange couplings. The averaged value of the lowest spin-gap energy is determined to be 722±2 GHz (34.7 K). We have also found a second spin-gap excitation at 1140 GHz (54.7 K), which indicates that the inter-dimer coupling is strong. Besides these modes, a number of gapped ESR absorptions are found and we propose that these excitations are caused by the localized nature of the excited state in the present system.

KEYWORDS: $SrCu_2(BO_3)_2$, spin gap, ESR, magnetic excitation, high magnetic field

Low-dimensional quantum spin systems with a finite spin gap have been the subject of intense and advanced research in this decade. One of the factors lies in the prominent progress of solid state chemistry, enabling a tailoring of various low-dimensional spin systems for the experimental verification of a concept brought about by theoretical study. Recently, the compound $SrCu_2(BO_3)_2$ has been added to the list of two-dimensional (2D) systems with a spin-gapped ground state.[1)] One prominent characteristic is that this material can be regarded as a model system with an exactly known ground state. $SrCu_2(BO_3)_2$ has a tetragonal unit cell and all Cu^{2+} ions are located at equivalent sites.[2)] In a $CuBO_3$ layer sandwiched by layers of Sr ions, a dimer unit is composed of a neighboring pair of planar rectangular CuO_4 and these dimers connect orthogonally by way of a triangular planar BO_3, providing a unique 2D network of $\boldsymbol{S} = 1/2$, as shown in the inset of Fig. 1. This 2D lattice is topologically equivalent to a 2D square lattice with additional alternating diagonal interactions, for which the direct product of the singlet pairs is the exact eigenstate, as proven by Shastry and Sutherland.[3)] This model for $SrCu_2(BO_3)_2$ can thus be considered a 2D analogue of the Majumdar-Ghosh model with some stringent condition.[4)] The role of the next-nearest-neighbor interaction in the $\boldsymbol{ac}$-plane $\boldsymbol{J}_2$, which brings a frustration into the system, has also been studied theoretically by Miyahara and Ueda.[5,6)] They estimated the intra-dimer coupling of $\boldsymbol{J} = 100$ K and the next-nearest-neighbor one of $\boldsymbol{J}_2 = 68$ K using the experimentally obtained Weiss temperature of -92.5 K and the energy gap of 30 K. It should be noted that the ratio $\boldsymbol{J}_2/\boldsymbol{J} = 0.68$ is just below the critical value of $\boldsymbol{J}_2/\boldsymbol{J} = 0.70$ between the spin-gap state and the Néel-ordered state. Thus, this material resides near the border between these two states.[6,7)]

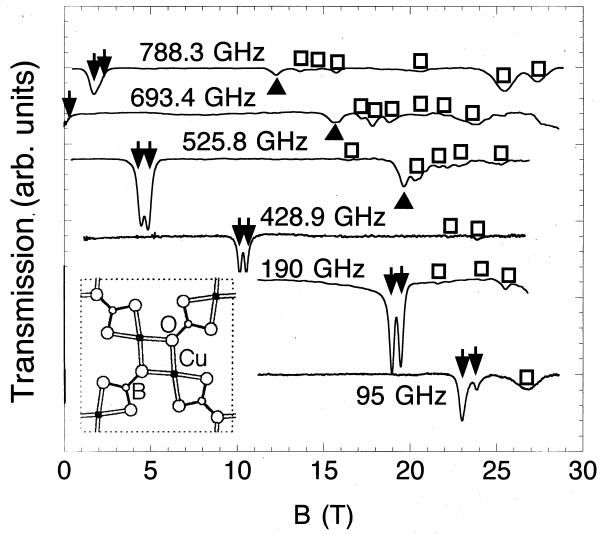

Fig. 1. Examples of ESR spectra at 1.6 K for $\boldsymbol{H} \parallel a$. Arrows indicate the two lowest triplets T1 and T2. Suffixes u and d indicate $S_z = +1$ and $S_z = -1$ branches, respectively. Closed triangles and open rectangles indicate the second lowest triplet and other multiple weak signals, respectively. The inset shows the schematic crystal structure in the $\boldsymbol{c}$-plane. The dotted line shows the unit cell.

Another interesting feature appears in the magnetization curve with quantized plateaux at one-quarter, one-eighth,[1)] and possibly one-tenth[8)] of the saturated moment. These plateaux have been realized due to the extremely localized nature of the low-lying excited triplets.[6)] This means that excited triplets cannot propagate freely in the 2D lattice. As a result, it is considered that these triplets organize a regular lattice composed of triplets.

Hence, it will be very interesting to study the field dependence of the magnetic excitation of this system. However, since the critical field is above 20 T, only a few methods can be applied to investigate the magnetic excitation in such high fields. Among the many different methods, ESR has established its unique status as a probe of magnetic excitation particularly to study its field variation.[9-11] Thus, we have performed a systematic study of the magnetic excitations of $SrCu_2(BO_3)_2$ by using a submillimeter-wave ESR.

Submillimeter-wave ESR measurements have been performed in pulsed magnetic fields up to 30 T. High-purity bulk single crystals of $SrCu_2(BO_3)_2$ were grown by the travelling solvent floating zone (TSFZ) method.[12] The grown materials were checked and the crystal axes were determined by the Laue X-ray photograph.

ESR spectra at 1.6 K are depicted in Fig. 1 for $\boldsymbol{H} \parallel a$. Among the many different kinds of ESR signals, a set of two resonance peaks marked by arrows shows characteristic frequency dependence. As the frequency is increased, the resonance field first decreases and then increases again at higher frequencies. The resonance fields are summarized as the frequency field diagram in Figs. 2(a) and 2(b) for $\boldsymbol{H} \parallel c$ and $\boldsymbol{H} \parallel a$, respectively. As shown in these figures, the above-mentioned ESR signals, marked by closed circles ($T1_u$ and $T1_d$) and closed rectangles ($T2_u$ and $T2_d$), are associated with a zero-field energy gap of about 720 GHz. This value is close to that estimated by different methods.[1, 8, 13-15] These findings indicate clearly that the two modes correspond to the transitions between the ground singlet state and the first excited triplet state (we call these modes singlet-triplet transition hereafter). As shown in Figs. 2(a) and 2(b), we have observed two branches of $S_z = +1$ and $S_z = -1$ for each triplet mode T1 or T2 (we use notations such as T1 when we treat $T1_u$ and $T1_d$ as a set of triplet). The $S_z = 0$ branch cannot be detected by our field-scanning ESR.

The lowest spin-gap excitations T1 and T2 exhibit a complicated structure. For $\boldsymbol{H} \parallel a$, a zero-field splitting exists between two branches of $S_z = +1$ and $S_z = -1$. The modes $T1_u$ and $T2_u$ or $T1_d$ and $T2_d$ are degenerated at zero field and the centers of $S_z = +1$ and $S_z = -1$ branches are identical between T1 and T2 modes. A small splitting observed at high fields between $T1_u$ and $T2_u$ or between $T1_d$ and $T2_d$ cannot be explained by the anisotropy of the $\boldsymbol{g}$-value in the $\boldsymbol{c}$-plane because all Cu sites are equivalent with respect to magnetic fields for $\boldsymbol{H} \parallel a$.[2] Thus, we infer that a small lattice distortion occurs at low temperatures, though detailed structural analysis at low temperatures is required to clarify this point. On the other hand, for $\boldsymbol{H} \parallel c$, no zero-field splitting exists between the two branches of $S_z = +1$ and $S_z = -1$, while two triplets T1 and T2 exhibit a splitting at zero field. These characteristic behaviors will be explained below by considering the anisotropic inter-dimer and intra-dimer exchange couplings. The slope of these modes for each field direction is nearly identical to that of the paramagnetic resonance signals indicated by dashed lines in Figs. 2(a) and 2(b). The $\boldsymbol{g}$-values are determined as $\boldsymbol{g}_a = 2.05$ and $\boldsymbol{g}_c = 2.28$ by the paramagnetic resonance peak positions at 25 K. From Figs. 2(a) and 2(b), we determine the average value of the lowest spin gap as 722±2 GHz (34.7 K).

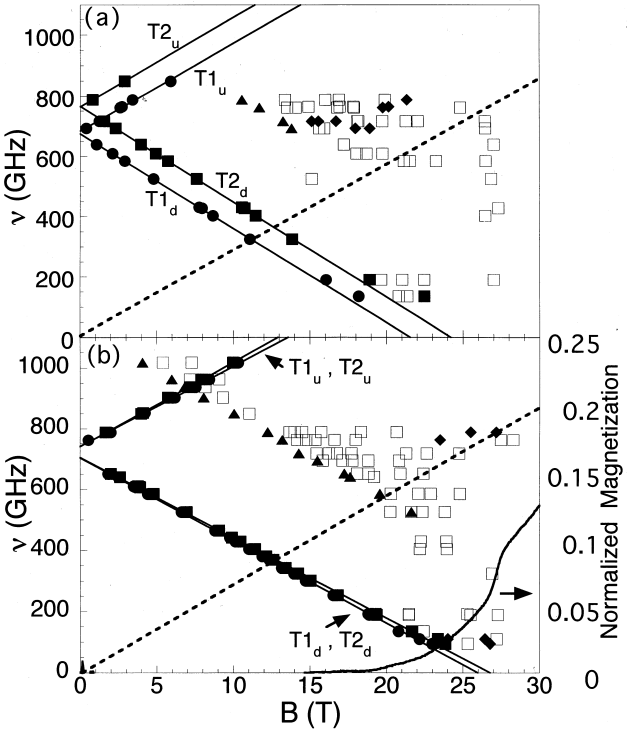

Fig. 2. The frequency-field diagrams at 1.6 K for $\boldsymbol{H} \parallel c$ (a) and for $\boldsymbol{H} \parallel a$ (b). Dashed lines indicate the position of paramagnetic resonance. Closed circles and closed rectangles indicate the two triplet modes T1 and T2. Closed triangles indicate the second lowest triplet. Closed diamonds and open rectangles are other strong and weak signals, respectively, as mentioned in the text. The magnetization curve of the single crystal measured at 0.5 K taken from ref. 8 is also plotted for $\boldsymbol{H} \parallel a$.

This assignment of T1 and T2 to the singlet-triplet transition is further confirmed by the temperature dependence of ESR spectra, as shown in Fig. 3. The intensity of the two peaks marked by arrows decreases as the temperature is increased. This behavior indicates that these signals are the transitions from the ground state of the system. As is well known, the ESR transition between the ground singlet state and the excited triplet state due to the mechanism of magnetic dipole transition is usually forbidden. However, the presence of a non-secular term such as the Dzyaloshinsky-Moriya (DM) interaction, non-equivalent $\boldsymbol{g}$-tensors or the anisotropic exchange interaction (AE) makes it possible to observe this transition by means of ESR. We speculate that the AE is the origin of the break down of the selection rule in $SrCu_2(BO_3)_2$ and the reason is discussed below.

Since each Cu is bridged by a planar CuO_4 unit which lies parallel in the $\boldsymbol{c}$-plane, we can expect that the crystal field on each Cu^{2+} ion exhibits a tetragonal symmetry and the principal axis is along the $\boldsymbol{c}$-axis. One of the evidences of the tetragonal crystal field is the anisotropy of the $\boldsymbol{g}$-value. The anisotropy of the $\boldsymbol{g}$-value in the $\boldsymbol{c}$-plane is less than 5% of that in the $\boldsymbol{ac}$-plane. This angular dependence is consistent with the tetragonal crystal field expected from the symmetry of the CuO_4 unit. In a tetragonal crystal field, we can also expect that $\boldsymbol{J}_{cc}$

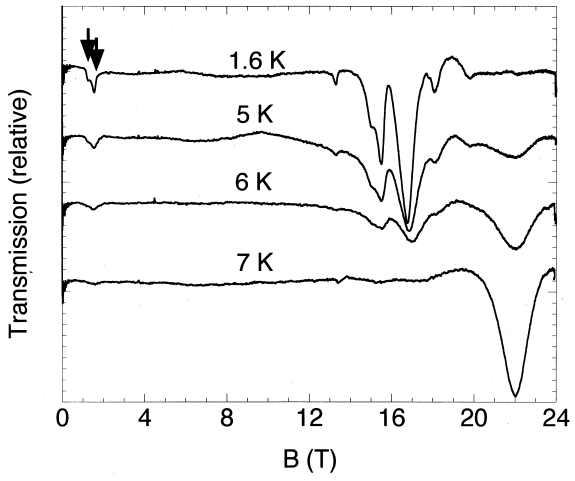

Fig. 3. Temperature dependence of ESR spectra at 716.7 GHz. Arrows indicate T1 and T2 modes.

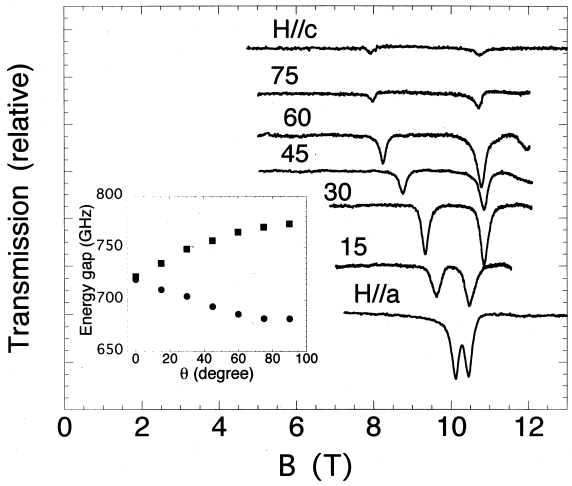

Fig. 4. A angular dependence of T1 and T2 modes at 1.6 K and at 428.9 GHz in the ac-plane. The number for each spectrum is the angle θ between magnetic field and the a-axis. The inset shows the angular dependence of the zero-field energy gaps of T1 (closed circles) mode and T2 (closed rectangles) mode.

deviates from $\boldsymbol{J}_{aa}$, where $\boldsymbol{J}_{cc}$ and $\boldsymbol{J}_{aa}$ are the components parallel and perpendicular to the $\boldsymbol{c}$-axis of the intra-dimer exchange coupling $\boldsymbol{J}$, respectively. As is well known, the order of AE can be estimated approximately by the relation AE $\sim (\Delta \boldsymbol{g}/\boldsymbol{g})^2 \boldsymbol{J}_i$, where $\Delta \boldsymbol{g}/\boldsymbol{g}$ is the anisotropy of the $\boldsymbol{g}$-value normalized by the average of $\boldsymbol{g}$, and $\boldsymbol{J}_i$ is the isotropic part of exchange constant. By using $\boldsymbol{g}_a = 2.05$, $\boldsymbol{g}_c = 2.28$ and $\boldsymbol{J}_i \approx \boldsymbol{J} = 100\,\mathrm{K}$, we evaluate AE$\sim$1 K. This value is comparable to the zero-field splitting of about 30 GHz between $S_z = +1$ and $S_z = -1$ branches in Fig. 2(b). To understand the difference in the zero-field splitting between $\boldsymbol{H} \parallel c$ and $\boldsymbol{H} \parallel a$ configurations, let us consider an isolated dimer of $S = 1/2$ coupled by an antiferromagnetic exchange interaction with exchange anisotropy. By diagonalizing the Hamiltonian of a dimer with such anisotropic exchange coupling, we can demonstrate that the splitting at zero field exists between $S_z = +1$ and $S_z = -1$ branches for $\boldsymbol{H} \perp c$ and that no splitting exists for $\boldsymbol{H} \parallel c$ between these two branches. This field-orientation dependence is consistent with the experimental results of the splitting between $S_z = 1$ and $S_z = -1$ branches shown in Figs. 2(a) and 2(b). Thus, we conclude that the AE is the origin of the above-mentioned splitting and this term makes the singlet-triplet transition allowable for ESR.

Next, let us discuss the parallel splitting of the lowest energy spin gap excitation for $\boldsymbol{H} \parallel c$ into the T1 and T2 modes. This splitting cannot be attributed to the difference of the $\boldsymbol{g}$-value because the splitting exists even at zero fields and both modes are parallel to each other, as shown in Fig. 2(a). Such a splitting can be expected when an inter-dimer interaction $\boldsymbol{J}'$ exists. Since the splitting depends on the field orientation, we speculate that the splitting is caused by the anisotropy of $\boldsymbol{J}'$ and is not related to the absolute total value of $\boldsymbol{J}'$. To confirm this point, we measured the angular dependence of two peaks T1$_d$ and T2$_d$, as shown in Fig. 4. By using the angular dependence of the $\boldsymbol{g}$-value, the zero-field energy of the two triplets is evaluated as a function of field orientation, as shown in the inset of Fig. 4. It should be noted that the splitting exhibits a sinusoidal angular dependence. Thus, we speculated that this parallel splitting is caused by the anisotropic inter-dimer exchange interaction.

When a finite $\boldsymbol{J}'$ exists, we can expect that the second excited state splits from the lowest triplet state due to $\boldsymbol{J}'$. In practice, the second lowest singlet-triplet transition is found and the energy gap is about 1140 GHz (see closed triangles in Figs. 2(a) and 2(b)). Since $\boldsymbol{J}_2 = 68\,\mathrm{K}$ is comparable to the intra-dimer coupling $\boldsymbol{J}$ in the present system, a theoretical calculation of the energy levels of the excited states is very difficult and a perturbative treatment may not be successful. Although it cannot be applied directly to the present case, it is useful to consider the energy level of the following simple $S = 1$ dimer model to understand why the second excited state is the triplet. When $\boldsymbol{J}' < \boldsymbol{J}$, we can treat two dimers coupled by $\boldsymbol{J}'$ as a dimer of two $S = 1$ spins. In this case, the ground state ($E = 0$), the first excited state ($E = \boldsymbol{J}'$) and the second excited state ($E = 3\boldsymbol{J}'$) are $S = 0$ singlet, $S = 1$ triplet and $S = 2$ quintet, respectively, where E is the energy of each level. More correctly, we have to include all four nearest-neighbored dimers. In both cases, however, the first excited state is the triplet as long as the condition $\boldsymbol{J}' < \boldsymbol{J}$ holds. Thus, we speculate that the second triplet branch is the transition between the ground state and the excited state in which the two triplets are coupled by $\boldsymbol{J}'$. The fact that the intensity of this transition increases monotonically with decreasing temperature indicates that this mode is the transition from the ground state. The weak intensity of the second triplet branch compared to that of the lowest triplet at 722$\pm$2 GHz can be understood because the former transition is caused by the simultaneous excitation of two dimers. It should be noted that the $S = 1$ dimer model is not realistic and that $\boldsymbol{J}'$ cannot be related to $\boldsymbol{J}_2$. It is essential to include all of the many-body interactions to evaluate the correct energy levels of the excited states theoretically. Experimentally, however, the second energy gap was also observed by neutron scattering experiments,[16] and the value of the energy gap is consistent

with the present result. Thus, we conclude that the existence of the second spin gap for both $\boldsymbol{H} \parallel c$ and $\boldsymbol{H} \parallel a$, is attributable to the large $\boldsymbol{J}'$ in the present system.

When we examine the frequency-field diagram shown in Figs. 2(a) and 2(b), we note that a number of ESR signals are observed besides the lowest and the second lowest energy modes of the singlet-triplet transition. We categorize these signals into the following two types: (1) strong ESR absorption appearing just below the critical field $\boldsymbol{H}_c$ marked by closed diamond, and (2) other weak ESR signals marked by open rectangles. To investigate the origin of the strong ESR mode (1), we measured the temperature dependence of the ESR spectra, as shown in Fig. 3. The signal located at 22 T is the transition in the excited states. The intensity of this peak is almost constant between 10–25 K and it decreases rapidly below 10 K. This behavior is completely different from that expected for a simple isolated dimer model and the details will be given in a separate paper. Since the intensity of all ESR peaks appearing around 15–17 T decreases as the temperature is increased, these signals are considered to be the excitations from the ground state. It should also be noted that the intensity of these peaks is much stronger than that of the singlet-triplet transition and is comparable to the signal observed at 22 T and at 7 K. Moreover, these signals are not related to the magnetic excitations at a plateau because the fields are well below $\boldsymbol{H}_c$, where the lowest triplet state intersects the singlet ground state. These findings indicate that the strong signals are related to the ground state but are not a forbidden transition, such as a singlet-triplet transition. Hence, we infer that the ground state of the system near the $\boldsymbol{H}_c$ is not a perfect nonmagnetic singlet state; i.e., part of the singlet is broken and, as a consequence, a magnetic ground state is recovered locally for the finite mixing between the ground singlet state and the excited states. In practice, the bending of modes $\mathrm{T1}_d$ and $\mathrm{T2}_d$ is observed above 15 T, as shown in Fig. 2(a) and the magnetization is non-zero even at 0.5 K in the field well below $\boldsymbol{H}_c$.[8)]

Finally, we discuss the origin of the weak signals marked by open rectangles. It appears that many of them lie almost parallel to the transition T1 or T2. This indicates that these ESR signals have a finite zero-field energy gap and thus, they are the transitions between the ground state and the excited state. We speculate that these weak absorptions are the localized multiple spin-gap excitations caused by the extremely localized nature of the excited state proposed theoretically.[6)] Usually, an excited triplet in the dimerized spin-gap system can propagate for the finite inter-dimer coupling and thus, a dispersion is observed. In the present system, a triplet excitation is extremely localized and its propagation is considerably suppressed. In this case, we expect that a dispersive mode may be replaced with a number of excitations which consist of nearly degenerated discrete energy levels. Namely, we can expect a state where triplets are coupled as dimer, trimer, quadramer, etc. In this case, the excitation energy of each level may be given by the sum of the formation energy of the isolated triplet, the interactions with other triplets located nearby and the Zeeman energy. This idea can explain why most of the weak ESR peaks appear above the $S_z = -1$ branch of the second lowest singlet-triplet transition marked by closed triangles. It also explains why the number of peaks increases when a field approaches to $\boldsymbol{H}_c$. It is because the number of surrounding triplets is increased around $\boldsymbol{H}_c$. As is well known, for the Ising system, such localized excitations are realized for their discrete energy levels. In practice, localized modes have been observed as a spin-cluster excitations.[17,18)] However, such a localized excitation has not been observed for the Heisenberg system. We propose that the present observation of the multiple spin-gap excitations is the manifestation of the extremely localized nature of the excited state in the Shastry and Sutherland model.

To summarize, we have directly observed singlet-triplet transition of $SrCu_2(BO_3)_2$. Two sets of well-defined triplet modes are found and the energy gaps are evaluated to be 722±2 GHz (34.7 K) and 1140 GHz (54.7 K). In addition to these transitions, we have also observed multiple spin-gap excitations, which may be realized by the extremely localized nature of the excited state.

Acknowledgements

This work was partly supported by a Grant-in-Aid from the Ministry of Education, Science, Sports and Culture, Japan.

1) H. Kageyama, K. Yoshimura, R. Stern, N. V. Mushnikov, K. Onizuka, M. Kato, K. Kosuge, C. P. Slichter, T. Goto and Y. Ueda: Phys. Rev. Lett. **82** (1999) 3168.
2) R. W. Smith and D. A. Keszler: J. Solid State Chem. **93** (1991) 430.
3) B. S. Shastry and B. Sutherland: Physica **108B** (1981) 1069.
4) C. K. Majumdar and D. K. Ghosh: J. Math. Phys. **10** (1969) 1399.
5) K. Ueda and S. Miyahara: J. Phys.: Condens. Matter. **11** (1999) L175.
6) S. Miyahara and K. Ueda: Phys. Rev. Lett. **82** (1999) 3701.
7) Z. Weihong, C. J. Hamer and J. Oitmaa: cond-mat/9811030.
8) H. Kageyama, K. Onizuka, T. Yamauchi, Y. Ueda, S. Hane, H. Mitamura, T. Goto, K. Yoshimura and K. Kosuge: to appear in J. Phys. Soc. Jpn.
9) H. Nojiri, H. Ohta, N. Miura and M. Motokawa: Physica B **246–247** (1998) 16.
10) S. Luther, H. Nojiri, M. Motokawa, M. Isobe and Y. Ueda: J. Phys. Soc. Jpn. **67** (1998) 3715.
11) B. Kurniawan, H. Tanaka, K. Takatsu, W. Shiramura, T. Fukuda, H. Nojiri and M. Motokawa: Phys. Rev. Lett. **82** (1999)1281.
12) H. Kageyama, K. Onizuka, T. Yamauchi and Y. Ueda: to appear in J. Cryst. Growth.
13) M. Takigawa: private communication.
14) H. Kageyama, M. Nohara, H. Suzuki, K. Onizuka, Y. Ueda and H. Takagi: preprint.
15) T. Room, U. Nagel, E. Lippmaa, H. Kageyama, K. Onizuka and Y. Ueda: *Proc. 22nd. International Conference for Low Temperature Physics*, August, 1999.
16) H. Kageyama, K. Onizuka, Y. Ueda, M. Nishi, N. Aso, T. Yoshihama, K. Kodama, K. Nukui and K. Kakurai: unpublished.
17) M. Date and M. Motokawa: Phys. Rev. Lett. **16** (1966) 1111.
18) J. B. Torrence Jr. and M. Tinkham: Phys. Rev. **197** (1969) 587, *ibid.* 595.